Complex Systems **3** (1989) 383–405

Cellular Automaton Model for Fluid Flow in Porous Media

Paul Papatzacos
Høgskolesenteret i Rogaland, Postboks 2557, Ullandhaug, 4001 Stavanger, Norway

Abstract. A cellular automaton model for the simulation of fluid flow in porous media is presented. A lattice and a set of rules are introduced, such that the flow equations in the continuum limit are formally the same as the equations for one-phase liquid flow in porous media. The model is valid in two as well as three dimensions. Numerical calculations of some simple problems are presented and compared with known analytical results. Agreement is within estimated errors.

1. Introduction

It is well known that the Navier–Stokes equation can be derived by two alternative methods, which may be called macroscopic and microscopic. The macroscopic method builds on the hypothesis that fluids are structureless continua and uses conservation laws of general validity [6]. The viscosity coefficients are introduced as constants to be determined by experiments. The microscopic approach, on the other hand, is based on the molecular structure of fluids and uses the framework of statistical physics [8]. The viscosity is here calculable in terms of the intermolecular potential.

There is an analogous division in the theory of flow in porous media and the Darcy equation. The macroscopic point of view starts with Darcy's law, which states that the rate of one-dimensional flow is proportional to the pressure gradient, and generalizes this law by introducing a permeability tensor. The components of this tensor are to be determined by experiments. The microscopic method is represented by an extensive literature (see for example [9] and references given there) where it is shown that the Darcy equation arises from an averaging out of Navier–Stokes flow by the pores and that the permeability tensor is in principle deducible from the pore geometry. The length scale is here microscopic only as far as the porous medium is concerned: the pores are visible but the fluid is structureless.

The recent paper by Rothman [7] on the cellular automaton simulation of flow in porous media is in the microscopic tradition. Using the FHP [3] triangular-lattice gas it shows how to estimate the permeability of almost

arbitrary pore geometries by introducing impermeable regions in the lattice. It is thus a framework for studying permeability.

The present paper is in the macroscopic tradition. A lattice and a set of rules are devised in such a way that the resulting lattice gas obeys an equation which is formally identical to the equation of motion of one phase flow in porous media. The coefficients of the lattice-gas equation of motion are adjustable so that one is able to match the corresponding coefficients of the equation to solve. This model is thus a framework for the numerical solution of a specific equation. The motivation for such a model is that some important problems are difficult to solve, either analytically or by standard numerical methods. Irregular boundaries, impermeable layers, large permeability contrasts between adjacent layers are some of the features of such problems.

Section 2 presents the equation governing one phase flow in porous media, which is the equation to simulate. The lattice-gas (lattice and rules) is presented in section 3. The calculations leading to the flow equation for the lattice gas, following the methods that have been used for simulating hydrodynamics [3,4,10], are shown in sections 4 and 5. Finally, sections 6 and 7 present numerical checks.

2. One phase flow in porous media

The differential equation for liquid flow at constant temperature in a porous medium [1] is essentially a mass conservation equation

$$\partial'_t(\varphi\varrho') + \partial'_i(\varrho' q_i) = S, \tag{2.1}$$

where ∂'_t and ∂'_i denote partial derivation with respect to time t' and coordinate $x'_i (i = 1, 2, 3)$. The summation convention is assumed and primed letters are used for those quantities which will eventually be scaled, reserving unprimed letters to their dimensionless counterparts to be introduced later on. S is the mass of fluid, injected (if positive) or removed (if negative) per unit time and per unit volume of the medium. Further, φ is the rock porosity, ϱ' is the fluid mass per unit volume, and q_i are the components of the so-called superficial or Darcy velocity, given by

$$q_i = -\mu^{-1} K_{ij}(\partial'_j p - \varrho' g_j). \tag{2.2}$$

Here μ is the fluid viscosity, p is the fluid pressure, K_{ij} is the permeability tensor, and g_j is the acceleration due to gravity with components $(0, -g, 0)$ if the second coordinate-axis is vertical and points upwards. (Such a placement of coordinate axes is convenient for the presentation of the rest of the paper. See section 3.)

For liquid flow at constant temperature one usually assumes [1] that ϱ' is a function of pressure exclusively and that the compressibility

$$\beta = \frac{1}{\varrho'} \frac{d\varrho'}{dp} \tag{2.3}$$

is a constant.

Equations (2.1–2.3) are usually combined into one equation for the pressure [1]. From the point of view of a cellular automaton simulation it is more interesting to have ϱ' as the dependent variable. With the assumption that $\varrho' = \varrho'(p)$ and using equation (2.3) one gets

$$\partial'_j \varrho' = \beta \varrho' \, \partial'_j p, \tag{2.4}$$

and combining this with equations (2.1) and (2.2) one obtains

$$\partial'_t \varrho' - (\varphi \mu \beta)^{-1} K_{ij} \partial'_i (\partial'_j p - \beta \varrho^2 g_j) = S \varphi^{-1}, \tag{2.5}$$

assuming that K_{ij}, φ, μ, and β are constants. The following assumptions about the permeability tensor usually allow one to model most cases of practical interest. It is symmetric, one of its principal axes is vertical, and it is isotropic in the horizontal direction. The second axis being vertical, these assumptions imply that

$$K_{ij} = 0 \quad (i \neq j), \qquad K_{11} = K_{33} \equiv k_h, \qquad K_{22} \equiv k_v,$$

so that the flow equation, equation (2.5), becomes

$$\varphi \mu \beta \partial'_t \varrho' - k_h (\partial'^2_1 + \partial'^2_3) \varrho' - k_v \partial'_2 (\partial'_2 \varrho' + \beta g \varrho'^2) = \mu \beta S. \tag{2.6}$$

It is appropriate, at this point, to scale the primed quantities by introducing a length scale L_0, a time scale T_0 and a density scale ϱ_0:

$$x'_i = L_0 x_i, \qquad t' = T_0 t, \qquad \varrho' = \varrho_0 \varrho. \tag{2.7}$$

The dimensionless flow equation is then

$$\partial_t \varrho - \mathcal{N}_h (\partial_1^2 + \partial_3^2) \varrho - \mathcal{N}_v \partial_2 (\partial_2 \varrho + \mathcal{N}_g \varrho^2) = \mathcal{N}_s, \tag{2.8}$$

where

$$\begin{aligned} \mathcal{N}_h &= k_h T_0 / (\varphi \mu \beta L_0^2), & \mathcal{N}_v &= k_v T_0 / (\varphi \mu \beta L_0^2), \\ \mathcal{N}_g &= g \varrho_0 L_0 \beta, & \mathcal{N}_s &= S T_0 / (\varphi \varrho_0). \end{aligned} \tag{2.9}$$

The dimensionless form of Darcy's law, equations (2.2), is

$$\begin{aligned} (L_0/T_0)^{-1} \varphi^{-1} q_1 &= -\mathcal{N}_h \, \varrho^{-1} \partial_1 \varrho, \\ (L_0/T_0)^{-1} \varphi^{-1} q_2 &= -\mathcal{N}_v \, (\varrho^{-1} \partial_2 \varrho + \mathcal{N}_g \varrho), \\ (L_0/T_0)^{-1} \varphi^{-1} q_3 &= -\mathcal{N}_h \, \varrho^{-1} \partial_3 \varrho, \end{aligned} \tag{2.10}$$

where L_0/T_0 has been used as a velocity scale, and where $\varphi^{-1}q_i$ is the interstitial velocity [1]. It is reminded that interstitial velocity plays the role, in a porous medium, of the usual fluid velocity.

The orders of magnitude of the dimensionless numbers defined by equations (2.9) are very dependent on the reservoir. The values given below for the rock and fluid parameters are meant to fix ideas.

$$\begin{array}{lllll} k_h & \approx & 10^{-12}\,\mathrm{m}^2, & k_v/k_h & \approx & 10^{-1}, \\ \beta & \approx & 10^{-9}\,\mathrm{Pa}^{-1}, & \mu & \approx & 10^{-3}\,\mathrm{Pa\,s}, \\ \varrho_0 & \approx & 10^{3}\,\mathrm{kg\,m}^{-3}, & g & \approx & 10\,\mathrm{m\,s}^{-2}, \\ \varphi & \approx & 0.3, & S & \approx & 1\,\mathrm{kg\,m}^{-3}\,\mathrm{s}^{-1}, \\ L_0 & \approx & 1\,\mathrm{m}, & T_0 & \approx & 1\,\mathrm{s}. \end{array}$$

One then finds:

$$\begin{array}{ll} \mathcal{N}_h \approx 3, & \mathcal{N}_v \approx 3\times 10^{-3}, \\ \mathcal{N}_g \approx 10^{-5}, & \mathcal{N}_s \approx 3\times 10^{-3}. \end{array} \tag{2.11}$$

The purpose of this paper is to find a cellular automaton model for simulating equation (2.8).

3. The lattice-gas rules

The lattice considered is cubic with grid length λ. The time step is denoted τ, and an elementary velocity c is introduced by

$$\lambda = c\tau.$$

The lack of isotropy encountered in the hydrodynamics of the HPP gas [3] will not arise here because velocity moments [4] larger than the second do not appear in the calculations. At each node six unit vectors $\mathbf{e}_\alpha$, $(\alpha = 1,\ldots,6)$ indicate the six possible directions for particle movements (figure 1). A particle with velocity $c\mathbf{e}_\alpha$ will be referred to as an $\mathbf{e}_\alpha$-particle. Greek indices are defined modulo 6 and the summation convention does not apply to them.

An appreciable number of problems can be studied in two dimensions and, moreover, the actual computer implementation is easier in two dimensions. It is thus desirable to have separate cellular automaton models for dimension two and for dimension three. There is no difference, for the model presented

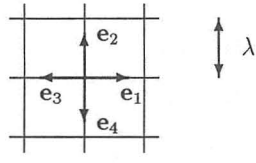

Figure 1: Definition of the lattice. Unit vectors $\mathbf{e}_5$ (pointing forward) and $\mathbf{e}_6$ (pointing backward) are not shown.

here, between two and three dimensions, other than appending two extra vectors to the two-dimensional case and applying the rules to these extra velocity directions. Since equation (2.8) shows that the vertical direction plays a special role because of the effect of gravity, vectors $\mathbf{e}_1$ to $\mathbf{e}_4$ will be considered to be in a vertical plane, with $\mathbf{e}_2$ pointing upwards. In such a manner a two-dimensional model, obtained by dropping the two directions $\mathbf{e}_5$ and $\mathbf{e}_6$, will retain the possibility of reproducing different horizontal and vertical permeabilities and of simulating gravity effects. The presentation in the rest of the paper is, as much as possible, independent of the number of dimensions.

Particle movements are governed by the following three rules.

1. There is at most one particle per state, where a state is specified by the position and the velocity. Thus there are at most $2d$ particles per lattice node, where d is the dimensionality of the space ($d = 2$ or 3).

2. A particle which is *alone* at a node at time t' is at one of the $2d$ neighboring nodes at time $t' + \tau$, with a velocity pointing away from the node it just left. The transition from direction $\mathbf{e}_\alpha$ to direction $\mathbf{e}_\beta$ takes place with probability $p_{\alpha\beta}$ (see figure 2). These probabilities satisfy

$$\sum_{\beta=1}^{2d} p_{\alpha\beta} = 1 \ (\alpha = 1, \ldots, 2d), \quad \sum_{\alpha=1}^{2d} p_{\alpha\beta} = 1 \ (\beta = 1, \ldots, 2d). \tag{3.1}$$

   The first equation is imposed by conservation of probability. The second expresses semi-detailed balance [4] and is a matter of choice; its importance for the present model will be pointed out in section 4.

3. With one exception, particles meeting at a node are not deflected. The exception concerns any *two-particle* collision involving an $\mathbf{e}_2$-particle. Such a collision results, with probability γ, in both velocities changing sign. See figure 3. This rule will be seen to give rise to a gravity term with the desired form.

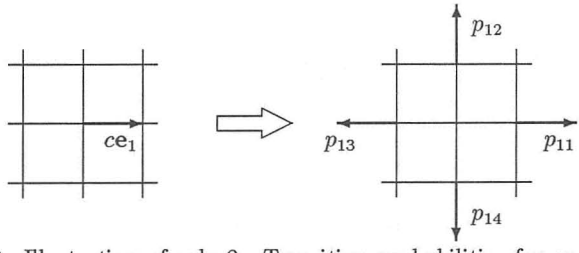

Figure 2: Illustration of rule 2. Transition probabilities for an $\mathbf{e}_1$-particle alone at a node. Transitions to directions 5 and 6 are not shown.

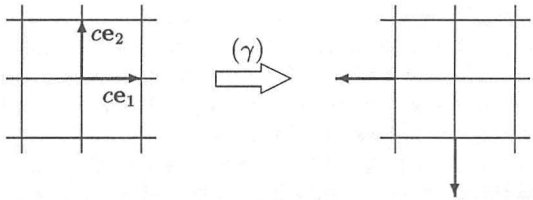

Figure 3: Illustration of rule 3. Any two-particle collision involving an $\mathbf{e}_2$-particle results, with probability γ, in an inversion of both velocities.

The rules are seen to be consistent. They conserve particle number but not momentum. An additional rule concerning particle creation or annihilation will be given in section 6.

4. The lattice Boltzmann equations and their equilibrium solution

Introducing $f_\alpha(\mathbf{r}', t')$, the mean population at node $\mathbf{r}'$, time t', and velocity direction $\mathbf{e}_\alpha$, the rules can be translated into what Frisch et al. [4] call the "lattice Boltzmann equations." These equations are here written directly and reference is made to [4] for their justification in terms of an ensemble average, using the Boltzmann assumption, of a set of microdynamical equations between Boolean variables. Keeping in mind that the Boltzmann assumption implies that many-particle distribution functions are products of one-particle distribution functions one finds:

$$f_\alpha(\mathbf{r}' + \lambda \mathbf{e}_\alpha, t' + \tau) - f_\alpha(\mathbf{r}', t') = \Omega_\alpha, \tag{4.1}$$

where

$$\Omega_\alpha / \Pi = \sum_{\beta=1}^{2d} \check{f}_\beta (p_{\beta\alpha} - \delta_{\beta\alpha}) + \gamma \check{f}_2 h_\alpha, \qquad (\alpha = 1, \ldots, 2d), \tag{4.2}$$

are calculated at $\mathbf{r}'$ and t'. The notation in equation (4.2) is as follows:

$$\check{f}_\alpha = f_\alpha / (1 - f_\alpha), \qquad \Pi = \prod_{\alpha=1}^{2d} (1 - f_\alpha), \tag{4.3}$$

and

$$\begin{array}{rcl} h_1 = -h_3 & = & \check{f}_3 - \check{f}_1, \\ h_2 = -h_4 & = & -\check{f}_1 - \check{f}_3 - \check{f}_5 - \check{f}_6, \\ h_5 = -h_6 & = & \check{f}_6 - \check{f}_5. \end{array} \tag{4.4}$$

If $d = 2$ then $\check{f}_5$ and $\check{f}_6$ are dropped from the expressions for h_2 and h_4.

It is easy to check that, as a consequence of conservation of probability (see the first set of equations (3.1)),

$$\sum_{\alpha=1}^{2d} \Omega_\alpha = 0, \tag{4.5}$$

which expresses particle conservation.

Equation (4.1) is valid when $\mathbf{r}'$ is at a node and t' is a multiple of τ. The transition to a continuum description is done by assuming that the f_α have appreciable variations only over a space scale $L \gg \lambda$ and a time scale $T \gg \tau$ so that it is possible to interpolate between the discrete points at which the f_α are originally defined. Actually one assumes that the interpolation gives functions that can be differentiated arbitrarily many times. The left-hand side of equation (4.1) can then be replaced by its Taylor expansion, to yield a differential form of the lattice Boltzmann equation:

$$\sum_{n=1}^{\infty} \frac{1}{n!}(\tau \partial'_t + \lambda e_{\alpha i} \partial'_i)^n f_\alpha = \Omega_\alpha. \tag{4.6}$$

The space and time variables are now scaled with the above quantities L and T:

$$x'_i = L x_i, \qquad t' = T t, \tag{4.7}$$

and it is assumed that

$$\lambda / L \equiv \varepsilon \ll 1. \tag{4.8}$$

Since the purpose of the model is to describe diffusion effects, the time-scale T must be such that [4]

$$\tau / T = \varepsilon^2. \tag{4.9}$$

Using equations (4.7–4.9) in equation (4.6), the latter takes the following dimensionless form:

$$\sum_{n=1}^{\infty} \frac{1}{n!}(\varepsilon^2 \partial_t + \varepsilon e_{\alpha i} \partial_i)^n f_\alpha = \Omega_\alpha. \tag{4.10}$$

Finally, fluid density is defined by

$$\rho(\mathbf{r}, t) = \sum_{\alpha=1}^{2d} f_\alpha(\mathbf{r}, t), \tag{4.11}$$

while fluid momentum, which is not a conserved quantity, is not used.

An equilibrium solution f_α^{eq} is now looked for, such that $\Omega_\alpha(f_\alpha^{eq}) = 0$, in the form of an expansion in powers of ε. This equilibrium solution will depend on the one conserved quantity, ρ. It is assumed in the present model that the fluid density is at most of order ε:

$$\rho = 2d\varepsilon\phi \tag{4.12}$$

where the factor $2d$ is included for convenience. Equation (4.11) shows that one may try $f_\alpha^{eq} = \varepsilon\phi$. The expressions defining Ω_α (equations (4.2–4.4)) show that, because of semi-detailed balance (the second set of equations (3.1)), this expression of f_α^{eq} is correct to order ε. One can thus set

$$f_\alpha^{eq} = \varepsilon\phi + \varepsilon^2\chi_\alpha + O(\varepsilon^3), \tag{4.13}$$

where, to satisfy equation (4.12),

$$\sum_{\alpha=1}^{2d} \chi_\alpha = 0. \tag{4.14}$$

(It will be seen later that terms of order ε^3 are not needed.) The χ_α are found by solving equations $\Omega_\alpha(f_\alpha^{eq}) = 0$ perturbatively to order ε^2. One finds that the χ_α satisfy

$$\sum_{\beta=1}^{2d} \chi_\beta(p_{\beta\alpha} - \delta_{\beta\alpha}) = 2\gamma(d-1)(\delta_{\alpha 2} - \delta_{\alpha 4})\phi^2. \tag{4.15}$$

Because of equations (3.1) the matrix with elements $p_{\alpha\beta} - \delta_{\alpha\beta}$ has rank $2d-1$. There are thus $2d$ independent equations in the set consisting of equations (4.14) and (4.15), which determines the $2d$ χ_α's uniquely. Note that the hitherto unspecified matrix $p_{\alpha\beta}$ must satisfy the condition that the rank of $p_{\alpha\beta} - \delta_{\alpha\beta}$ is $2d-1$. The opposite case is equivalent to the existence of spurious conservation laws. The calculation of the χ_α is deferred to section 5.2, where a special form for the matrix $p_{\alpha\beta}$ is introduced.

5. The perturbation solution and the flow equation

5.1 The perturbation solution

Reference is made to [4] and [10] for a justification of the calculations which now follow. A solution to the differential Boltzmann equation (4.10) is sought by perturbing around the equilibrium solution, i.e., by setting

$$f_\alpha = f_\alpha^{eq} + \varepsilon\psi_\alpha^{(1)} + \varepsilon^2\psi_\alpha^{(2)} + O(\varepsilon^3), \tag{5.1}$$

and by requiring that the correction terms do not modify the density:

$$\sum_{\alpha=1}^{2d} \psi_\alpha^{(1)} = 0, \tag{5.2}$$

$$\sum_{\alpha=1}^{2d} \psi_\alpha^{(2)} = 0. \tag{5.3}$$

Combining equations (4.13) and (5.1) one finds, for the left-hand side of equation (4.10):

$$\begin{aligned}\sum_{n=1}^{\infty}\frac{1}{n!}(\varepsilon^2\partial_t+\varepsilon e_{\alpha i}\partial_i)^n f_\alpha &= \varepsilon^2 e_{\alpha i}\partial_i(\phi+\psi_\alpha^{(1)})+\varepsilon^3[\partial_t(\phi+\psi_\alpha^{(1)})\\ &+ e_{\alpha i}\partial_i(\chi_\alpha+\psi_\alpha^{(2)})+\tfrac{1}{2}e_{\alpha i}e_{\alpha j}\partial_i\partial_j(\phi+\psi_\alpha^{(1)})]\\ &+ O(\varepsilon^4),\end{aligned} \tag{5.4}$$

where the terms of order ε^4 involve terms in the expansion of f_α which are of order ε^3 (see equation (5.1)). To order ε, the right-hand side of equation (4.10) is

$$\Omega_\alpha=\varepsilon\sum_{\beta=1}^{2d}\psi_\beta^{(1)}(p_{\beta\alpha}-\delta_{\beta\alpha})+O(\varepsilon^2).$$

This must vanish identically. Accounting for equations (5.2) and remembering that $p_{\alpha\beta}-\delta_{\alpha\beta}$ has rank $2d-1$, one then finds that

$$\psi_\alpha^{(1)}=0. \tag{5.5}$$

With this simplification and using equation (4.15), the right-hand side of equation (4.10) becomes, to order ε^2,

$$\Omega_\alpha=\varepsilon^2\sum_{\beta=1}^{2d}\psi_\beta^{(2)}(p_{\beta\alpha}-\delta_{\beta\alpha})+O(\varepsilon^3). \tag{5.6}$$

Equating this to the right-hand side of equation (5.4), and using equation (5.5), one sees that the $\psi_\alpha^{(2)}$ are found by solving

$$\sum_{\beta=1}^{2d}\psi_\alpha^{(2)}(p_{\beta\alpha}-\delta_{\beta\alpha})=e_{\alpha i}\partial_i\phi \tag{5.7}$$

together with equations (5.3). Finally, the macrodynamical or flow equations [4,10] are found by summing the ε^3-term on the right-hand side of equation (5.4) over all values of α and equating the result to zero. Using equation (5.5) and

$$\sum_{\alpha=1}^{2d}e_{\alpha i}=0$$

one finds the following flow equation:

$$\partial_t\phi+\tfrac{1}{2d}\sum_{\alpha=1}^{2d}e_{\alpha i}\partial_i(\chi_\alpha+\psi_\alpha^{(2)})+\tfrac{1}{4d}\sum_{\alpha=1}^{2d}e_{\alpha i}e_{\alpha j}\partial_i\partial_j\phi=0, \tag{5.8}$$

where the χ_α and $\psi_\alpha^{(2)}$ are implicitly given in terms of ϕ by equations (4.14) and (4.15) and equations (5.3) and (5.7). Explicit expressions are given in the next subsection, after the introduction of a particular $p_{\alpha\beta}$-matrix.

5.2 A special transition matrix $p_{\alpha\beta}$

A special matrix $p_{\alpha\beta}$ is introduced, with elements depending on three parameters and general enough to cover all cases of interest. Remembering that the plane of the four unit vectors $\mathbf{e}_1, \ldots, \mathbf{e}_4$ is vertical, that vector $\mathbf{e}_2$ points upwards, and that $\mathbf{e}_5$ and $\mathbf{e}_6$ are appended whenever a three-dimensional model is desired, a transition matrix with the following properties is considered. (The properties are written for the three-dimensional case.)

The differences between the probabilities of forward and backward scattering only depend on whether the original direction of motion is horizontal or vertical:

$$\begin{aligned} p_{11} \;-\; p_{13} &= p_{66} - p_{65} = p_{33} - p_{31} = p_{55} - p_{56} \equiv \delta_h, \\ p_{22} \;-\; p_{24} &= p_{44} - p_{42} \equiv \delta_v. \end{aligned} \tag{5.9}$$

The probabilities for scattering in a transverse direction are independent of the original direction of motion:

$$p_{\alpha\beta} = \varpi \text{ for all } \alpha \text{ and } \beta \text{ such that } \mathbf{e}_\alpha \cdot \mathbf{e}_\beta = 0.$$

The transition matrix has then the following form:

$$(p_{\alpha\beta}) = \begin{pmatrix} H_+ & \varpi & H_- & \varpi & \varpi & \varpi \\ \varpi & V_+ & \varpi & V_- & \varpi & \varpi \\ H_- & \varpi & H_+ & \varpi & \varpi & \varpi \\ \varpi & V_- & \varpi & V_+ & \varpi & \varpi \\ \varpi & \varpi & \varpi & \varpi & H_+ & H_- \\ \varpi & \varpi & \varpi & \varpi & H_- & H_+ \end{pmatrix} \tag{5.10}$$

where, for two dimensions, the last two columns and the last two lines must be dropped, and where

$$H_\pm = (1 \pm \delta_h)/2 - (d-1)\varpi, \qquad V_\pm = (1 \pm \delta_v)/2 - (d-1)\varpi. \tag{5.11}$$

Note that equations (3.1) are satisfied and that the transition matrix is now symmetric (detailed balance [4]). The requirement that the matrix elements be in the interval $[0,1]$ imposes the limitation that the triplet $(\delta_h, \delta_v, \varpi)$ be inside or on the surface of a pyramid defined by $|\delta_h| \leq 1$, $|\delta_v| \leq 1$, and $0 \leq \varpi \leq [2(d-1)]^{-1}$. Further, the requirement that the matrix $p_{\alpha\beta} - \delta_{\alpha\beta}$ be of rank $2d-1$ excludes the base ($\varpi = 0$) of this pyramid (see figure 4).

With this transition matrix the expressions for the χ_α (found by solving equations (4.14) and (4.15)) and for the $\psi_\alpha^{(2)}$ (found by solving equations (5.3) and (5.7)) are

$$\chi_\alpha = -\tfrac{2\gamma(d-1)}{1-\delta_v}\phi^2(\delta_{\alpha 2} - \delta_{\alpha 4}), \qquad (\alpha = 1, \ldots, 2d), \tag{5.12}$$

$$\psi_\alpha^{(2)} = -\kappa_\alpha e_{\alpha i}\partial_i\phi, \qquad (\alpha = 1, \ldots, 2d), \tag{5.13}$$

where it is reminded that greek indices are not summed, and where

$$\begin{aligned} \kappa_1 = \kappa_3 = \kappa_5 = \kappa_6 &= (1-\delta_h)^{-1}, \\ \kappa_2 = \kappa_4 &= (1-\delta_v)^{-1}. \end{aligned} \tag{5.14}$$

The resulting flow equation now follows.

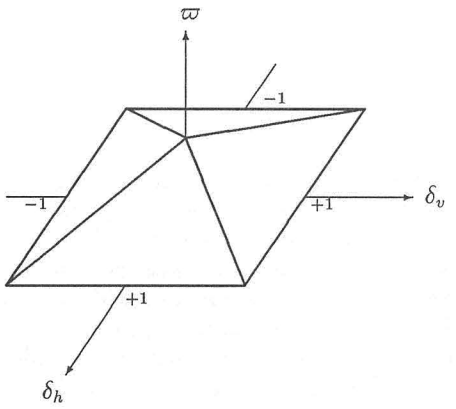

Figure 4: Allowed values of $(\delta_h, \delta_v, \varpi)$ are inside and on the surface of the pyramid, except its base. The height of the pyramid is $[2(d-1)]^{-1}$.

5.3 The flow equation

The flow equation is found by using equations (5.12) and (5.13), together with

$$\sum_{\alpha=1}^{2d} e_{\alpha i} e_{\alpha j} = 2\delta_{ij},$$

in equation (5.8). Keeping in mind that the unit vectors along the coordinate axes x_1, x_2, and x_3 are, respectively, $\mathbf{e}_1$, $\mathbf{e}_2$, and $\mathbf{e}_5$, and that the two-dimensional model is obtained by dropping coordinate x_3 and unit vector $\mathbf{e}_5$, one finds:

$$\partial_t \phi - \frac{1+\delta_h}{4(1-\delta_h)} \partial_1^2 \phi - \frac{1+\delta_v}{4(1-\delta_v)} \partial_2 \left(\partial_2 \phi + \frac{4\gamma}{1+\delta_v} \phi^2 \right) = 0 \tag{5.15}$$

in two dimensions, and

$$\partial_t \phi - \frac{1+\delta_h}{6(1-\delta_h)} (\partial_1^2 + \partial_3^2) \phi - \frac{1+\delta_v}{6(1-\delta_v)} \partial_2 \left(\partial_2 \phi + \frac{8\gamma}{1+\delta_v} \phi^2 \right) = 0 \tag{5.16}$$

in three dimensions. For a direct comparison of these equations with the dimensionless equations of section 2, a scale ϕ_0 of order of magnitude 1 is introduced for ϕ,

$$\phi = \phi_0 \Phi. \tag{5.17}$$

Equations (5.15) and (5.16) can now be written

$$\partial_t \Phi - \mathcal{C}_h^{(d)} [\partial_1^2 + (d-2)\partial_3^2] \Phi - \mathcal{C}_v^{(d)} \partial_2 (\partial_2 \Phi + \mathcal{C}_g^{(d)} \Phi^2) = 0, \tag{5.18}$$

where $d = 2$ or 3 and

$$\begin{aligned} \mathcal{C}_h^{(d)} &= (2d)^{-1}(1+\delta_h)(1-\delta_h)^{-1}, \\ \mathcal{C}_v^{(d)} &= (2d)^{-1}(1+\delta_v)(1-\delta_v)^{-1}, \\ \mathcal{C}_g^{(d)} &= 4(d-1)\gamma(1+\delta_v)^{-1}\phi_0. \end{aligned} \tag{5.19}$$

Equation (5.18) is now identical to equation (2.8) with no source term, $d = 2$ corresponding to ϱ being independent of x_3. Equations (5.19) show that it is *a priori* possible to reproduce any set of values $\mathcal{N}_h$ and $\mathcal{N}_v$ by choosing δ_h and δ_v. It is also possible to reproduce $\mathcal{N}_g$ as long as its order of magnitude is less than about 1, which should be possible in a wide variety of cases according to the numerical value shown in equations (2.11).

Note that care has to be taken in simulating so-called layered reservoirs where k_v and hence $\mathcal{N}_v$ take different values in different intervals along the vertical axis. The values of $\mathcal{C}_v^{(d)}$ are adjusted by choosing different δ_v's in different layers. To obtain identity between $\mathcal{N}_g$ and $\mathcal{C}_g^{(d)}$ one must choose different γ's in different layers in such a way that $\gamma(1+\delta_v)^{-1}$ remains constant throughout.

The velocity has not played any role in the calculations because momentum is not conserved by the automaton rules. However, it is interesting to use the definition of velocity u_i (as an ensemble average or mean velocity per node [4,10])

$$\rho u_i = c \sum_{\alpha=1}^{2d} f_\alpha e_{\alpha i}$$

to obtain the expression of velocity in this model. Using the expression for f_α (equations (5.1), (5.5), (5.12), and (5.13)), together with equations (4.12), (5.17), and (5.19) one finds, with $d = 3$:

$$\begin{aligned} (L/T)^{-1}u_1 &= -[3(1-\delta_h)]^{-1}\,\Phi^{-1}\partial_1\Phi, \\ (L/T)^{-1}u_2 &= -[3(1-\delta_v)]^{-1}\,(\Phi^{-1}\partial_2\Phi + 4\gamma\Phi), \\ (L/T)^{-1}u_3 &= -[3(1-\delta_h)]^{-1}\,\Phi^{-1}\partial_3\Phi. \end{aligned} \tag{5.20}$$

These expressions do not give the correct expression for the Darcy velocity. Indeed, eliminating gravity and setting the permeabilities to zero by putting $\gamma = 0$ and $\delta_h = \delta_v = -1$ (see equations (5.18) and (5.19)), one sees that expressions (5.20) do not give zero velocity. The defining equations (5.9) show that, when $\delta_h = \delta_v = -1$, particles with no nearest neighbors jump back and forth between two adjacent nodes; there are similar "cycles" involving two or more nearest neighbors. The macroscopic velocity field of a lattice gas in this state, calculated on a single history as a space and time average with scales L and T, is zero. This suggests the following definition of the dimensionless Darcy velocity v_i:

$$v_i = (L/T)^{-1}[u_i(\delta_h, \delta_v, \gamma) - u_i(-1,-1,0)]. \tag{5.21}$$

Using expressions (5.20) one then finds

$$v_1 = -\mathcal{C}_h^{(3)}\,\Phi^{-1}\partial_1\Phi,$$
$$v_2 = -\mathcal{C}_v^{(3)}\,(\Phi^{-1}\partial_2\Phi + \mathcal{C}_g^{(3)}\Phi), \tag{5.22}$$
$$v_3 = -\mathcal{C}_h^{(3)}\,\Phi^{-1}\partial_3\Phi.$$

Comparing equations (5.18) and (5.22) with equations (2.8) and (2.10) one sees that v_i has the correct expression.

It may be objected to this derivation that the Darcy velocity given by expressions (2.10) vanishes with the horizontal and vertical permeabilities, even with a nonzero gravity term, so that the renormalizing term in equation (5.21) should be $u_i(-1,-1,\gamma)$. However, equations (5.18) and (5.19) show that the gravity term for the lattice gas is proportional to $\gamma/(1+\delta_v)$ so that it is necessary to set $\gamma = 0$ when $\delta_v = -1$. Also, the argument can be carried out as a limiting procedure, where δ_h and δ_v are made to approach -1, so as to avoid a confrontation with the fact that values $\delta_h = -1$ and $\delta_v = -1$ are not allowed (see figure 4).

6. First numerical check: Two-dimensional flow without gravity

In this section, the cellular automaton will be checked against an analytical calculation. A model is set up in such a way that it is possible to solve the diffusion equation analytically, which means that very simple boundaries and boundary conditions are chosen. The boundary is a square, with the condition that no flow takes place across it. A source, at the center of the square, injects fluid at a (preferably) constant rate, starting with no fluid at zero time. The simulation of such a situation with a cellular automaton presents no problems as far as the no-flow boundary is concerned. Particle creation at a constant rate is, however, not straightforward because of the rule that there is at most one particle per state.

The additional rule concerning creation, and the resulting modification of equation (5.15), will be considered first. Let the source be located at node $\mathbf{r}'_s$ and let $\sigma_\alpha(\mathbf{r}',t')$ be the probability of creating an $\mathbf{e}_\alpha$-particle at $\mathbf{r}'$ and t' ($\sigma_\alpha(\mathbf{r}',t') \neq 0$ only if $\mathbf{r}' = \mathbf{r}'_s$). Equations (4.1) and (5.18) become, respectively,

$$f_\alpha(\mathbf{r}' + \lambda\mathbf{e}_\alpha, t' + \tau) - f_\alpha(\mathbf{r}', t') = \Omega_\alpha + \sigma_\alpha,$$

and

$$\partial_t\Phi - \mathcal{C}_h^{(2)}\partial_1^2\Phi - \mathcal{C}_v^{(2)}\partial_2^2\Phi = \sigma/(4\varepsilon^3), \tag{6.1}$$

where

$$\sigma = \sum_{\alpha=1}^{4}\sigma_\alpha. \tag{6.2}$$

In equation (6.1), $\sigma \neq 0$ only inside a square region with side ε and centered at $\mathbf{r}'_s$. The order of magnitude of σ can be estimated by referring to the assumption that the fluid density is at most of order ε (see equation (4.12)). The number of particles created after T/τ time steps is about $(T/\tau)\sigma$. The first particles created have traveled a distance of the order of $\sqrt{(T/\tau)}$ so that the average particle density created is of the order of $(T/\tau)\sigma/(\sqrt{(T/\tau)})^2 = \sigma$. Since this must be at most of order ε one may set

$$\sigma = \varepsilon\nu, \tag{6.3}$$

so that the right-hand side of equation (6.1) is $\nu/(4\varepsilon^2)$ where ν, like s, is different from 0 only inside a square region with side ε and centered at $(x_1 = x_{1s}, x_2 = x_{2s})$. It follows that, when $\varepsilon \to 0$, equation (6.1) can be written

$$\partial_t\Phi - \mathcal{C}_h^{(2)}\partial_1^2\Phi - \mathcal{C}_v^{(2)}\partial_2^2\Phi = (\nu/4)\delta(x_1 - x_{1s})\delta(x_2 - x_{2s}), \tag{6.4}$$

where $\delta(x)$ is the Dirac delta function.

As already mentioned, the lattice is assumed to be square. Let the length of its side be $N\lambda$ where N is odd so that there is a central node where particle creation takes place. The automaton can be run when a choice has been made for δ_h, δ_v, ϖ, and for $\sigma = \varepsilon\nu$. The boundaries of the square are such that all particles arriving there are reflected (with an initially empty lattice, there will never be any particles tangential to the boundary). The central node creates an $\mathbf{e}_\alpha$-particle with a probability $\varepsilon\nu/4$ if such a particle does not already occupy the node. Particle densities are then calculated and compared with the analytical solution of equation (6.4).

The properties of the analytical solution are now briefly examined. It is convenient for simplicity to introduce the following notation:

$$p = \sqrt{\mathcal{C}_v^{(2)}\mathcal{C}_h^{(2)}}, \qquad r = \sqrt{\mathcal{C}_v^{(2)}/\mathcal{C}_h^{(2)}}. \tag{6.5}$$

The fact that one must work with a low density of particles, together with the rule that a particle is created at the central node only if a particle of the same type does not already occupy the node, means that a constant rate of creation cannot be exactly maintained so that it is necessary to consider a time-dependent ν on the right-hand side of equation (6.4). With $\Phi = 0$ at zero time one can then write the solution as

$$\Phi(\xi,\eta,\theta) = \frac{1}{4p}\int_0^\theta \nu(\theta')G(\xi,\eta,\theta-\theta')\,d\theta', \tag{6.6}$$

where the Green function G is given by [2]

$$\begin{aligned} G(\xi,\eta,\theta) = 1 \;&+\; 2\sum_{n=1}^{\infty} e^{-4\pi^2 n^2\theta/r}\cos(n\pi\xi) + 2\sum_{n=1}^{\infty} e^{-4\pi^2 n^2\theta r}\cos(n\pi\eta) \\ &+\; 4\sum_{m=1}^{\infty}\sum_{n=1}^{\infty} e^{-4\pi^2(m^2/r+n^2 r)\theta}\cos(m\pi\xi)\cos(n\pi\eta). \end{aligned} \tag{6.7}$$

In these equations, the space coordinates ξ and η have their origin at the central node and vary between -1 and $+1$ (see figure 5). The time variable θ,

when related to the number of time steps t'/τ (see section 4), is

$$\theta = \frac{t'/\tau}{N_\theta}, \qquad N_\theta = N^2/p \tag{6.8}$$

which shows that the appropriate unit of time, in number of time steps, is N_θ.

Particle densities obtained during the automaton run must be compared with numerical values given by equation (6.6). Actually, the calculation of particle densities involves an averaging of particle numbers in both space and time. In terms of the coordinates (ξ, η, θ) introduced above, let Δ_ξ be the linear dimension of the space averaging region and Δ_θ be the time averaging interval. In lattice terms there will be $N^2\Delta_\xi^2$ sites in a space averaging region and, according to equation (6.8), there will be $N^2\Delta_\theta/p$ time steps in a time averaging interval. In the automaton runs described below there are two space averaging regions, centered at $(\xi = 1/2, \eta = 0)$ (labeled E in figure 5) and at $(\xi = 0, \eta = 1/2)$ (labeled N in the same figure).

Time averaging is done as follows. One first chooses a final time $\theta = \theta_f$, a multiple of the averaging interval Δ_θ. This determines, through equation (6.8), the maximum number of time steps the automaton is to be run, namely $\theta_f N^2/p$. (It will be shown below that the choice of θ_f can not be made arbitrarily.) Space averages are registered at each time step, over a number of time steps corresponding to Δ_θ, namely $N^2\Delta_\theta/p$, and the mean value and standard deviation are calculated. This standard deviation is assumed to be an estimate of the "experimental error" attached to the mean value. In principle both the mean value and the standard deviation should be calculated by repeating the experiment many times and recording the space average at a given time. The standard deviation calculated as described above is some-

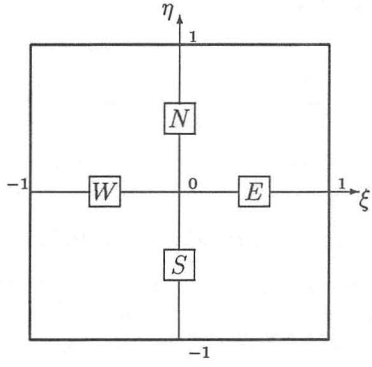

Figure 5: Lattice and averaging regions (E, N, W, S) for numerical check without gravity effect. The lattice is square, with side $(2M + 1)\lambda$. The averaging regions are squares, centered halfway to the edges, and with side $(2m + 1)\lambda$.

what larger than its correct value because the mean values vary with time inside the time averaging interval.

The mean value itself could be assumed to be an estimate of particle density at the center of the space averaging region and in the middle of the time averaging region, to be compared with the numbers given by the analytical expression, equation (6.6). It is preferable, however, to compare the above mean value with the analytical expression obtained by averaging equation (6.6) over the corresponding space and time regions. This allows to choose values for Δ_ξ and Δ_θ which are not too small.

It remains to define the ν-function in equation (6.6). The automaton runs are started with a "requested" creation probability $\sigma = \sigma_{req}$ (i.e., $\nu = \nu_{req}$ according to equation (6.3)). The expected number of particles created between time θ and $\theta + \Delta_\theta$ is $N^2\Delta_\theta\sigma_{req}/p$. The actual number of particles created varies, however, because of statistical fluctuations but also because of the rule that a particle is created only if a particle of the same type does not already exist at the central node. For example, in one of the runs presented below, $\sigma_{req} = 0.05$ and the interval Δ_θ corresponds to 1020 time steps, so that the expected number of particles created per Δ_θ-interval is 51. The actual numbers registered in successive Δ_θ-intervals are, however,

$$50, 36, 49, 52, 40, 53, 40, 54, \ldots .$$

To account for these variations, equation (6.6) is written

$$\Phi(\xi, \eta, \theta) = \Phi_0 \int_0^\theta \hat{\nu}(\theta') G(\xi, \eta, \theta - \theta')\, d\theta', \tag{6.9}$$

$$\Phi_0 = \nu_{req}/(4p), \qquad \hat{\nu}(\theta) = \nu(\theta)/\nu_{req} \tag{6.10}$$

where $\hat{\nu}(\theta)$ is defined by

$$\hat{\nu}(\theta) = \hat{\nu}_k \quad \text{for} \quad (k-1)\Delta_\theta \le \theta \le k\Delta_\theta,$$

and

$$\hat{\nu}_k = \frac{\text{Number of particles created for } (k-1)\Delta_\theta \le \theta \le k\Delta_\theta}{N^2\Delta_\theta\sigma_{req}/p}.$$

Referring to the example already mentioned, the first numbers in the $\hat{\nu}_k$ sequence are

$$50/51, 36/51, 49/51, 52/51, 40/51, 53/51, 40/51, 54/51, \ldots .$$

Returning now to the averaging of the analytical expression over space and time and referring to equation (6.9), a function $\langle\Phi\rangle_k$ is defined as the average of Φ/Φ_0 in region E of figure 5 and in the interval $[(k-1)\Delta_\theta, k\Delta_\theta]$:

$$\langle\Phi\rangle_k = \frac{1}{\Delta_\theta}\int_{(k-1)\Delta_\theta}^{k\Delta_\theta} d\theta \frac{1}{\Delta_\xi^2}\int_{-\Delta_\xi/2}^{\Delta_\xi/2} d\eta \int_{(1-\Delta_\xi)/2}^{(1+\Delta_\xi)/2} d\xi \int_0^\theta \hat{\nu}(\theta') G(\xi, \eta, \theta - \theta')\, d\theta'. \tag{6.11}$$

The calculation of this expression with the Green function given by equation (6.7) is straightforward but tedious. The details are not given here.

Figure 5 shows four space averaging regions, labeled E, N, W, and S, centered halfway from the lattice center to the edges, and with side equal to Δ_ξ. Because of symmetry, the analytical particle density averaged, at a given time, in region E can be compared to the average number of particles, at the corresponding time step, in region $E+W$ (or in region $E+W+N+S$ if $r = 1$). If $r \neq 1$, the average number of particles in region $N+S$ can, because of the form of the Green function, be compared to the above mentioned analytical average provided $1/r$ is substituted to r in equation (6.7).

Finally, the space-time averages of particle numbers obtained from running the automaton must be normalized in a manner which is comparable to the normalization of $\langle\Phi\rangle_k$, i.e. by dividing them by Φ_0. Recalling equation (4.12), one must also divide by 4ε, so that the normalized and averaged particle number is

$$\begin{aligned} \langle P\rangle_k^R &= (\text{Space-time average of particle numbers})/P_0, \\ P_0 &= \sigma_{req}/p, \end{aligned} \tag{6.12}$$

where k refers to the interval $[(k-1)\Delta_\theta, k\Delta_\theta]$, and R is either $E+W$ or $N+S$ (when $r = 1$, R is $E+W+N+S$). Note that neither $\langle\Phi\rangle_k$ nor $\langle P\rangle_k$ directly depend on ε. This parameter is, however, indirectly present through σ_{req} which must be at most of order ε.

The results of two experiments are shown in figures 6 and 7. The parameter values for each experiment are given in table 1.

Note that the lattice sizes are chosen so that N^2 is approximately 10^4 for one case and 10^5 for the other. These figures are plots of $\langle P\rangle_k$ and $\langle\Phi\rangle_k$ against θ, each average being allocated to the value of θ which is in the middle of the time-averaging interval. While $r = 1$ in figure 6, figure 7 shows the result of a run with $r = 0.1$ (meaning that $\mathcal{C}_v^{(2)}/\mathcal{C}_h^{(2)} = 0.01$).

The final value of θ, θ_f, can not be arbitrarily large because the model assumes low particle densities so that the particle creation process must be stopped when the density reaches some number less than one. It will now be shown that the requirement of a maximum overall particle density of order ε determines the upper bound of θ_f up to a factor of order 1. The

Figure 6		Figure 7	
$N = 101$	$\mathcal{C}_h^{(2)} = 1$	$N = 317$	$\mathcal{C}_h^{(2)} = 10$
$\delta_h = 3/5$	$\mathcal{C}_v^{(2)} = 1$	$\delta_h = 39/41$	$\mathcal{C}_v^{(2)} = 1/10$
$\delta_v = 3/5$	$r = 1$	$\delta_v = -3/7$	$r = 1/10$
$\varpi = 1/10$	$p = 1$	$\varpi = 1/82$	$p = 1$
$\sigma_{req} = 0.05$	$N_\theta = 10201$	$\sigma_{req} = 0.05$	$N_\theta = 100489$
$\Delta_\xi = 0.2$,	$\Delta_\theta = 0.1$	$\Delta_\xi = 0.2$,	$\Delta_\theta = 0.1$

Table 1: Parameter values for the automaton runs illustrated in the indicated figures.

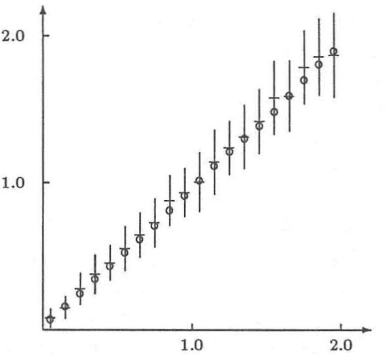

Figure 6: Plot of the space and time averaged particle-numbers given by equation (6.12) ((–) with "error bars" extending one standard deviation above and one below), and of the corresponding analytical averages given by equation (6.11) (o) versus time θ. The parameter values are given in table 1. In particular, $r = 1$.

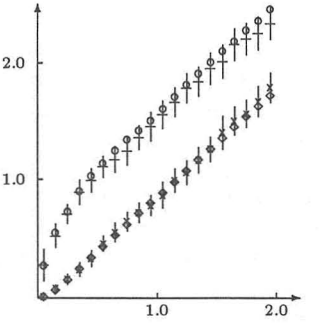

Figure 7: Plot of the space and time averaged particle-numbers given by equation (6.12) ((–) for the E + W averages and (×) for the N + S averages, with "error bars" extending one standard deviation above and one below), and of the corresponding analytical averages given by equation (6.11) ((o) and ($\diamond$)) versus time θ. The parameter values are given in table 1. In particular, $r = 0.1$.

number of time steps necessary to reach θ_f being $N^2\theta_f/p$, the approximate total number of particles created is $N^2\theta_f\sigma_{req}/p$, so that the maximum overall density is $\theta_f\sigma_{req}/p$. With $\sigma_{req} = \varepsilon\nu_{req}$ one sees that

$$\theta_{f\,max} \propto p/\nu_{req},$$

where the proportionality factor is of order 1. Thus, for given p, the way to explore large times is to reduce the particle creation probability. In both automaton "experiments" presented above one has in mind a value of ε equal to 0.1 and the value of θ_f corresponds to a maximum overall particle density equal to 0.1.

All other parameters being constant, the standard deviations are roughly proportional to $N^{-1/2}$. It should also be noted that, a value of θ_f being given, calculation time on a sequential computer is proportional to N^4 (N^5) for a to-dimensional (three-dimensional) simulation. A power of 2 (3) accounts for the number of nodes and an additional power of 2 accounts for the number of time steps.

Equations (5.18) and (5.19) show that the probability for right angle scattering, ϖ, is not "measurable," i.e., it does not appear in the numerical coefficients. The particular choice of ϖ in any automaton run is thus only limited by the fact that the point of coordinates $(\delta_h, \delta_v, \varpi)$ must be inside the pyramid of figure 4. In the automaton runs referred to in this and the next section, ϖ has been arbitrarily chosen halfway up from the point $(\delta_h, \delta_v, 0)$ on the pyramid base, to the point $(\delta_h, \delta_v, \varpi_{max})$ on the pyramid side.

It should finally be noted that the flow equations without the gravity term are linear. The quantity denoted above by $\langle P \rangle$, given by a cellular automaton run, is then a numerical solution of equation (6.1) where Φ is replaced by $\Phi - \Phi_i$ (with Φ_i an arbitrary constant, for example an initial value of Φ). It is also a numerical solution of the same equation with Φ replaced by $\Phi_i - \Phi$ and σ replaced by $-\sigma$, meaning that one has a practical way of simulating depletion by an automaton run with particle creation and a subsequent change of sign in the interpretation of the results.

7. Second numerical check: One-dimensional flow with gravity

As in the previous section, an automaton run is checked against an analytical solution of equation (5.18), where $d = 2$ and Φ is assumed independent of x_1, so that it becomes

$$\partial_t \Phi - -\mathcal{C}_v^{(2)} \partial_2 (\partial_2 \Phi + \mathcal{C}_g^{(2)} \Phi^2) = 0. \tag{7.1}$$

This equation is nonlinear and no analytical solution is known. It is however possible to chose the start and boundary conditions in such a way that the solution evolves to a time independent function, $\Phi^\infty(x_2)$. One can then compare the long time prediction of the automaton with $\Phi^\infty(x_2)$. A possible set of such start and boundary conditions is the following:

$$\Phi = 1 \quad \text{at} \quad x_2 = 0, \tag{7.2}$$

$$\Phi = 0 \quad \text{at} \quad x_2 = N\varepsilon, \tag{7.3}$$

$$\Phi = 0 \quad \text{at} \quad t = 0. \tag{7.4}$$

It is reminded that the automaton lattice is square, with side $N\lambda$, which explains the right-hand side of equation (7.3). Function Φ^∞ is the solution to equations (7.1) (without the ∂_t-term), (7.2), and (7.3). The differential equation is of the Riccati type and one finds [5]

$$\Phi^\infty = \frac{\tan[a(1-\xi)]}{\tan a}, \tag{7.5}$$

where

$$\xi = x_2/(N\varepsilon) \tag{7.6}$$

and a is the solution of the transcendental equation

$$a \tan a = \mathcal{C}_g^{(2)} N\varepsilon = 4\varepsilon\phi_0 \frac{\gamma N}{1+\delta_v}. \tag{7.7}$$

On the right-hand side of this last equation, ϕ_0 is a scale for Φ (see equation (5.17)). Since Φ is set equal to 1 at the lower boundary by equation (7.2), the product $4\varepsilon\phi_0$ is, in lattice terms, the particle density at the lower boundary. Thus the automaton is run with reflecting right and left boundaries, a lower boundary with a constant particle density and an upper boundary with zero particle density. The condition at the upper boundary is easily implemented by annihilating all particles arriving there. The condition at the lower boundary is managed as follows. At the end of each time step, after the rules for particle movement have been applied, all particles are removed from the lower boundary and then, at preselected sites (say at each tenth site from the left, for a lattice with 100 sites on a side) particles of random types are created.

To compare the automaton output with equation (7.5) it is necessary to know the time scale of the solution of equation (7.1). An estimate of this time scale can be obtained by linearizing the equation, i.e., setting $\mathcal{C}_g^{(2)} = 0$. The solution of the linear equation, with start and boundary conditions given by equations (7.2–7.4), is [2]

$$\Phi^{lin} = 1 - \xi - \frac{2}{\pi} \sum_{n=1}^{\infty} (n)^{-1} e^{-n^2\pi^2\theta} \sin(n\pi\xi),$$

where ξ is defined by equation (7.6) and (compare with equation (6.8))

$$\theta = \frac{t'/\tau}{N_\theta}, \qquad N_\theta = N^2/\mathcal{C}_v^{(2)}. \tag{7.8}$$

Φ^{lin} is very nearly time-independent as soon as θ reaches the value 1 because of the exponential factors in the sum. It is therefore assumed that the automaton stabilizes, except for statistical fluctuations, for all time steps larger than $2N_\theta$.

A square lattice with $N = 100$ sites on a side has been chosen, together with constant particle density at the lower boundary $4\varepsilon\phi_0 = 0.1$, and $\mathcal{C}_v^{(2)} = 1$. This implies $N_\theta = 10^4$. Apart from that, two cases are presented with different scattering probabilities, as shown in table 2. Particle averages are calculated in space with $\Delta_\xi = 0.1$ and normalized through division by the particle density at the lower boundary ($4\varepsilon\phi_0$). Each space average is recorded for all time steps, starting at time step number 2×10^4 ($\theta = 2$) and ending at time step number 4×10^4 ($\theta = 4$). Mean values and standard deviations are calculated and the mean values are compared to the values given by

Figure 8	Figure 9
$\delta_h = 3/5$	$\delta_h = 0$
$\delta_v = 3/5$	$\delta_v = 3/5$
$\varpi = 1/10$	$\varpi = 1/10$
$\gamma = 1$	$\gamma = 1/2$

Table 2: Parameter values for the automaton runs illustrated in the indicated figures.

equation (7.5). Actually, since the space averaging region Δ_ξ is appreciably large, the comparison is done with

$$\langle \Phi \rangle_\ell = \frac{1}{\Delta_\xi} \int_{(\ell-1)\Delta_\xi}^{\ell\Delta_\xi} \Phi^\infty(\xi)\, d\xi = \frac{1}{\Delta_\xi a \tan a} \ln \frac{\cos[a(1-\ell\Delta_\xi)]}{\cos[a(1-(\ell-1)\Delta_\xi]}. \quad (7.9)$$

The space averaging intervals are numbered from the bottom ($\ell = 1$) to the top ($\ell = 1/\Delta_\xi$) of the lattice.

The results are shown in figures 8 and 9, where each space averaged value is allocated to the ξ-coordinate in the middle of the interval. There is agreement to within one standard deviation for most points.

8. Conclusions

A cellular automaton model for the simulation of one-phase liquid flow in porous media has been derived, and a set of simple checks has been presented. The simulations were done with FORTRAN programs on a MicroVax 3500. It took somewhat more than a CPU-hour to produce the data for figure 6 and about five days to produce the data for figure 7. More effective simulations

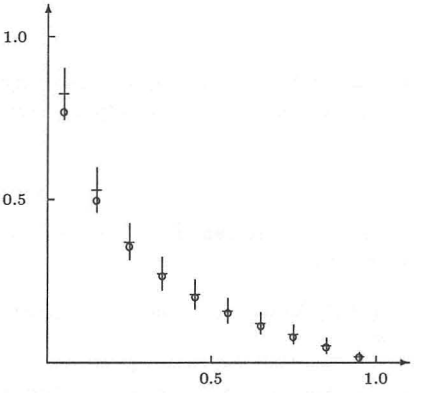

Figure 8: Plot of the space averaged particle numbers ((–), with "error bars" extending one standard deviation above and one below), and of the corresponding analytical averages given by equation 7.9 (o), versus coordinate ξ. The parameter values are given in table 2. In particular, $\gamma = 1$.

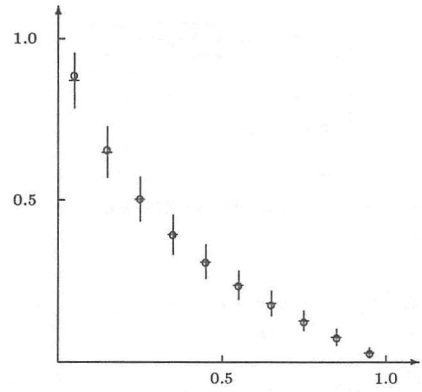

Figure 9: Plot of the space averaged particle numbers ((–), with "error bars" extending one standard deviation above and one below), and of the corresponding analytical averages given by equation 7.9 (o), versus coordinate ξ. The parameter values are given in table 2. In particular, $\gamma = 1/2$.

are in preparation, using parallel-C on a transputer card fitted to a personal computer. The purpose of these simulations is to explore some of the possibilities and limitations of the model. The possibility of three-dimensional simulation, for example, remains to be tested. The most obvious limitation of the model is its requirement of low densities. This limitation is especially illustrated in the examples presented in section 6 where simulation time is limited by the necessity to stop particle creation so as to remain in the low density regime.

Acknowledgments

I would like to thank Jens Feder for a most inspiring lecture on cellular automata, and Svein Skjæveland for expert help concerning porous media.

References

[1] K. Aziz and A. Settari, *Petroleum Reservoir Simulation* (Applied Science Publishers, London, 1979).

[2] H.S. Carslaw and J.C. Jaeger, *Conduction of Heat in Solids* (Clarendon Press, Oxford, 1959).

[3] U. Frisch, B. Hasslacher, and Y. Pomeau, "Lattice-gas automata for the Navier–Stokes equation," *Physical Review Letters*, **56** (1986) 1505–1508.

[4] U. Frisch, D. d'Humière, B. Hasslacher, P. Lallemand, Y. Pomeau, and J.-P. Rivet, "Lattice gas hydrodynamics in two and three dimensions," *Complex Systems*, **1** (1987) 649–707.

[5] E.L. Ince, *Ordinary Differential Equations* (Dover, New York, 1956).

[6] L.D. Landau and E.M. Lifshitz, *Fluid Mechanics* (Pergamon Press, Oxford, 1959).

[7] D.H. Rothman, "Cellular-automaton fluids: A model for flow in porous media," *Geophysics*, **53** (1988) 509–518.

[8] W.G. Vincenti and C.H. Kruger, Jr., *Introduction to Physical Gas Dynamics* (Robert E. Krieger Publishing Company, Malabar, Florida, 1965).

[9] S. Whitaker, "Flow in porous media I: A theoretical derivation of Darcy's law," *Transport in Porous Media*, **1** (1986) 3–25.

[10] S. Wolfram, "Cellular automaton fluids 1: Basic theory," *Journal of Statistical Physics*, **45** (1986) 476–526.